

Room temperature state-independent experimental test of quantum contextuality in solid state system

Xin-Yu Pan*, Gang-Qin Liu, Yan-Chun Chang and Heng Fan*

¹*Beijing National Laboratory for Condensed Matter Physics, Institute of Physics, Chinese Academy of Sciences, Beijing 100190, China*

*e-mail: xypan@aphy.iphy.ac.cn; hfan@iphy.ac.cn;

Quantum mechanics implies that not all physical properties can be simultaneously well defined, such as the momentum and position due to Heisenberg uncertainty principle. Some alternative theories have been explored, notably the non-contextual hidden variable theories in which the properties of a system have pre-defined values which are independent of the measurement contextual. However, the Kochen-Specker theorem ¹ showed that such non-contextual hidden variable theories are in conflict with quantum mechanics. Recently, a state-independent inequality satisfied by non-contextual hidden variable theories and violated by quantum mechanics is proposed in the simplest three-state system (a qutrit) by the least 13 projection measurement rays ². Here, we report an experimental demonstration of the violation of this inequality. This provides a state-independent experimental test of quantum contextuality, for the first time in solid state system, by a natural qutrit of nitrogen-vacancy center in diamond at room temperature.

The question of whether quantum phenomena can be explained by non-contextual hidden

variable theories has a long history ^{3,4}. Non-contextuality means that the measured value of an observable is independent of its own measurement and other co-measurable observables that are measured previously or simultaneously. This is in consistent with our experience in everyday lives. However, as proved by Kochen and Specker ¹, and also by Bell ⁵, the non-contextual hidden variable theories cannot reproduce quantum mechanics because quantum theory predicts that the outcomes depend on the context of measurement. This is proven either by the violation of Bell type inequalities since of the quantum nonlocality or by a logical contradiction between the local hidden variable predictions and those of quantum mechanics. The violation of Bell type inequalities depends on specified quantum entanglement state. The state-independent Kochen-Specker theorem is proven by a logical contradiction which applies to systems with dimension of Hilbert space larger than three.

The proof of Kochen-Specker theorem involves initially 117 observables in a qutrit system which is the simplest system capable of manifesting the quantum contextuality ¹. The number of observables involved in the proof is reduced gradually to 31 rays for state-independent case ^{6,7} and 5 rays for state-dependent case ⁸. Recently, Yu and Oh ² provide a state-independent proof with only 13 rays for a qutrit, which is optimal ⁹. The contradiction in this proof involves a Yu-Oh inequality which is consistent with non-contextual hidden variable theories but should be violated by any quantum states predicted by quantum mechanics. Additionally, the system only involves a single qutrit which is dimension three and is thus indivisible, so the contradiction cannot result from entanglement.

The quantum contextuality is continuously tested experimentally in two quantum bits (qubits) system by using photons ¹⁰, neutrons ^{11,12}, ions ¹³, ensembles of nuclear magnetic resonance ¹⁴. In a qutrit system, the state-dependent ⁸ experimental test is performed by single photons ¹⁵. The newly proposed Yu-Oh scheme is just realized experimentally also by photons ¹⁶. In this work, we report an experimental test of quantum contextuality, for the first time in solid-state system, by nitrogen-vacancy (NV) center in diamond at room temperature. Our experimental results strongly agree with quantum contextuality manifested in a state-independent characteristic.

A NV center comprises a substitutional nitrogen atom instead of a carbon atom and an adjacent lattice vacancy in diamond, which provides an electronic spin ^{17,18}. The electronic spin of NV center in diamond can be individually addressed, optically polarized, manipulated and measured with optical and microwave excitation. Since those properties and its long coherence time, the NV center system stands out as one of the most promising solid state systems as quantum information processors ^{19–23} and as a high-sensitivity magnetometer ^{24,25}.

The electronic ground state of the NV center is a spin triplet, which has zero magnetic moment $m_s = 0$ corresponding to state $|0\rangle$, and it exhibits a zero field splitting, defining the \hat{z} axis of the electron spin. By applying a magnetic field, the state splits into two magnetic sub-levels $m_s = \pm 1$ corresponding to $|1\rangle, |-1\rangle$, respectively, which allow selective microwave excitation. A qubit of NV center, which involves $m_s = 0$ and a single spin transition to either $m_s = 1$ or $m_s = -1$, has been widely demonstrated in various quantum information and interferometry schemes. A qutrit is a superposed three level state which will involve all three energy levels of

the electronic spin in a NV center. The precise control of an arbitrary qutrit in NV center is also demonstrated experimentally in a quantum information processing scheme in our group ²⁷. This provides a perfect experimental setup to test quantum contextuality of Yu-Oh scheme ², for a large variants of quantum states to illustrate the state-independent property.

The Yu-Oh proof of quantum contextuality involves arbitrary qutrits and 13 projection measurement rays ². For a given basis $\{|0\rangle, |1\rangle, |-1\rangle\}$ which are realized by three electronic spin energy levels of a NV center in our experiment, $m_s = 0, \pm 1$, the 13 normalized rays are represented as rank-1 qutrit projectors $\hat{r} = |r\rangle\langle r|$ in which $|r\rangle = a|0\rangle + b|1\rangle + c|2\rangle$ (see the Methods section). Suppose a_v are outcomes corresponding to those 13 observables, $a_u a_v$ are the correlations, it is shown ² that an inequality should be satisfied by non-contextual hidden variable theories, even though the usual Kochen-Specker value assignment does exist for those 13 rays,

$$\sum_u a_u - \frac{1}{4} \sum_{\langle u, v \rangle} a_u a_v \leq 8, \quad (1)$$

where $\langle u, v \rangle$ denotes all 24 compatible pairs of observables (see Fig.1 and the Methods section). On the other hand, this inequality should be violated by quantum mechanics since it is expected by quantum theory that $\sum_u a_u - \frac{1}{4} \sum_{\langle u, v \rangle} a_u a_v = 25/3 \approx 8.33$, no matter what kind of quantum states are measured.

In NV center system, the experimental test of quantum contextuality is to prepare arbitrary qutrits, measure 13 observables and 24 correlations for each qutrit. The aim is to find whether the inequality (1) is violated or not in a state-independent nature. The experiment is carried out in type IIa sample diamond (nitrogen concentration $\ll 1$ ppm), most of the atoms (^{12}C , natural

abundance of 98.9%) have no nuclear spin, result in a very pure spin bath and thus the NV electron spin has long enough coherence time such that the manipulation and readout of the qutrit is not affected by decoherence. But due to the hyperfine interaction with the host nitrogen nuclear spin, each of the electron spin state splits into three sub levels, and it is not sufficient to manipulate all the three sub-states by a single pulse. Fortunately, we can polarize the nuclear spin by adding an external magnetic field of about 500 Gauss along NV symmetry axis ²⁸. This magnetic field also lifts the degeneration between $m_s = \pm 1$ states. In Fig. 2 (b) we plot the optically detected magnetic resonance (ODMR) spectral of this center. The sharp dip at frequency of 1480.6 MHz and 4259.3 MHz are corresponding to the $|0\rangle \leftrightarrow |-1\rangle$ and $|0\rangle \leftrightarrow |1\rangle$ transitions. Fig. 2 (d) presents typical Rabi oscillation of this center. The perfect oscillation reveals that the microwave pulse can control the electron spin with high fidelity. The 532nm laser beam is modulated by an acousto-optic modulation (AOM) and then reflected to the objective by a galvanometer, which control the focus position on the sample. The fluorescence of $|0\rangle$ state is about 30% brighter than the $|1\rangle$ state, so the spin state of NV center can be readout by applying a short laser (0.3 μ s) pulse and recording the excited fluorescence at the same time.

Two microwave sources are used with different frequencies: MW1 and MW2. MW1 frequency is resonant with the transition $m_s=0 \leftrightarrow m_s=+1$, and MW2 with $m_s=0 \leftrightarrow m_s=-1$, which can create superposed states of $|0\rangle$ with $|1\rangle$ or $|-1\rangle$, respectively. The electron spin is firstly polarized into state $|0\rangle$ by laser pulse of duration 3.5 μ s followed by 5 μ s waiting. Then the combination of two microwaves, MW1 and MW2, will let us prepare an arbitrary qutrit in superposition form by controlling the duration of MW1 and MW2, see Methods for detail.

Experimentally, we prepare 13 pure qutrits $|r\rangle$ corresponding to 13 projectors as presented in Methods section. Other types of qutrits can be similarly prepared without any experimental difficulty since the same techniques can be used as those in preparing the 13 pure qutrits. With arbitrary qutrits prepared, the scheme of measurement is the same: measure 13 observables and 24 pairs of correlations. Experimentally, we realize each measurement of the 13 observables by a qutrit rotation such that the projector $|r\rangle\langle r|$ can be transformed to $|0\rangle\langle 0|$, which is realized by applying either MW1 or MW2 or both, followed by a readout of the intensity of florescence corresponding to the population in state $|0\rangle$ by normalization. The readout of state can be by two Rabi oscillations to fit the relative percentages between $|0\rangle$ and $|\pm 1\rangle$, then the form of the superposed qutrit can be found, see Methods. The scheme of measuring 24 correlations can be by measuring the joint probabilities or by multiplication the outcomes of compatible observables, see Methods

Our experiment results are presented in Fig.4. Each experimental data is the averaged value which is repeated for around 10,000 times. We have 13 pure states prepared, for each input state, Fig.4(a) shows the theoretical value of outcomes of 13 observables, Fig.4(b) are experiment results, within error rate 2%, experimental results agree exactly with theoretical results. Thus a simpler Yu-Oh version inequality involving only four h observables² is clearly violated. Fig.4 (c) shows three examples corresponding to three prepared pure states, the 13 outcomes of observables and the correlations agree well with theoretical expectation. Our results are summarized in Fig.4 (d), clearly for each prepared state, the inequality (1) is violated. The results ranges from around 8.1 to 8.5, the reason that some results are larger than theoretical value 8.33 is that, the measured outcomes are fitted with standard Rabi oscillations, so the error fluctuations can be on both directions.

Still the violation of (1) is convincing.

In this work, we observe that the inequality (1) is clearly violated thus the state-independent quantum contextuality is confirmed experimentally in a natural qutrit of nitrogen-vacancy center of diamond at room temperature. This real qutrit may close the possible loophole appeared in such as photonic systems induced by the post-selection technique. This represents the first experimental test of quantum contextuality in solid-state system, and provides new evidences in a most fundamental form that quantum mechanics is contextual.

Methods

Yu-Oh proof of quantum contextuality. Explicitly, the 13 rays take the forms corresponding to vectors (a, b, c) for $|r\rangle = a|0\rangle + b|1\rangle + c|2\rangle$ as shown in Fig.1 (c). The orthogonality relationships among the 13 rays are schematically represented in Fig.1(a). Correspondingly, we can define a set of 13 observables, $\hat{A}_v = 1 - 2\hat{r}_v$, where $\hat{r}_v \in \{\hat{z}_k, \hat{y}_k^\sigma, \hat{h}_k, \hat{h}_0\}$, $\sigma = \pm, k = 1, 2, 3$. When \hat{A}_u, \hat{A}_v are commuting, i.e., $|r_u\rangle$ and $|r_v\rangle$ are orthogonal, they are co-measurable (compatible) observables so that their correlation is well defined in quantum mechanics. In contrast, it is always well defined in a non-contextual hidden variable theory regardless of whether they are compatible or not, so that each outcome a_v of observable \hat{A}_v always takes values ± 1 . In quantum theory for the density operator ρ of an arbitrary quantum state, the outcome of an observable is, $a_v = \langle \hat{A}_v \rangle = \text{Tr}(\rho \hat{A}_v)$, and the correlation is, $a_u a_v = \langle \hat{A}_u \hat{A}_v \rangle = \text{Tr}(\rho \hat{A}_u \hat{A}_v)$, provided they are compatible. Then different results are expected from non-contextual hidden variable theories and quantum

mechanics depending on whether the inequality (1) is satisfied or violated. So the experimental test is only to check this inequality.

Preparation of arbitrary qutrits and readout. After initialization of the electron spin to $|0\rangle$, two channels of resonant microwave pulses are applied to manipulate the spin state. They are generated by individual source and timing controlled by individual RF switches, and then combined together to a 16 Watt amplifier. The amplified microwave signal is then delivered to the sample by a 20 μm copper wire which is mounted on the diamond surface. For each of the microwave pulses, its phase φ determines the rotation axis and the pulse duration t_{MW} determines the rotation angle. E.g. if we apply a MW1 pulse to state $|0\rangle$, and define $\theta = 2\pi t_{MW}/T$ with T being the duration of one circle of Rabi oscillation for MW1, then the result state is $\cos \frac{\theta}{2}|0\rangle + e^{i\varphi} \sin \frac{\theta}{2}|1\rangle$. This operation equals to rotate the state with θ angle around an axis in X-Y plane, where the angle between the rotation axis and X-axis is φ .

The readout is by measuring the intensities of fluorescence by two Rabi oscillations and fit the data to those two curves. Define P_1 and P_2 to represent the percentage of $|0\rangle$ among $\{|0\rangle, |1\rangle\}$ subspace and $\{|0\rangle, |-1\rangle\}$ subspace. By fitting the two Rabi curves we can extract P_1 and P_2 , together with the normalization condition we get the projection result: $P = \frac{P_1 P_2}{P_1 + P_2 - P_1 P_2}$. The projection results of 25 measurements for each state are combined together to calculate the 24 pairs of correlations.

Measurement of 24 correlations. The 24 pair correlations involved in the inequality (1) can be written in the form as $\langle \hat{A}_u \hat{A}_v \rangle = P_{(A_i=1, A_j=1)} + P_{(A_i=-1, A_j=-1)} - P_{(A_i=1, A_j=-1)} - P_{(A_i=-1, A_j=1)}$.

For an orthogonal set of rays $\{b_i, b_j, b_k\}$ which constitutes a complete basis as shown in Fig.1. We remark that ray b_k may not necessarily be within the existing 13 rays in Yu-Oh scheme. We have $P_{(b_i=1)} + P_{(b_j=1)} + P_{(b_k=1)} = 1$, so four terms on the right hand side of the above equation can be rewritten respectively as, $P_{(A_i=1, A_j=1)} = P_{(b_i=0, b_j=0)} = P_{(b_k=1)}$; $P_{(A_i=-1, A_j=-1)} = P_{(b_i=1, b_j=1)} = P_{(b_i=1|b_j=1)}P_{(b_j=1)}$; and $P_{(A_i=1, A_j=-1)} = (1 - P_{(b_i=1|b_j=1)})P_{(b_j=1)}$; $P_{(A_i=-1, A_j=1)} = (1 - P_{(b_j=1|b_i=1)})P_{(b_i=1)}$. In the last three equations, $P_{(b_i=1|b_j=1)}$ means the projection of ray $|b_j\rangle$ on b_i , which are actually orthogonal to each other. So the correlations are also realized by projective measurement. Alternatively, we can measure $\langle \hat{A}_u \hat{A}_v \rangle$ in a framework of quantum theory, such that the outcomes of $\langle b_i b_j \rangle$ is the square root of a multiplication of expectation values of b_i, b_j , and the projective measurement of state $|b_j\rangle$ on projector b_i . Those two methods give same result experimentally.

1. Kochen, S. & Specker, E. P. The problem of hidden variables in quantum mechanics. *J. Math. Phys.* **17**, 59 (1967).
2. Yu, S. X. & Oh, C. H. State-Independent Proof of Kochen-Specker Theorem with 13 Rays. *Phys. Rev. Lett.* **108**, 030402 (2012).
3. Einstein, A., Podolsky, B. & Rosen, N. Can quantum-mechanical description of physical reality be considered complete? *Phys. Rev.* **47**, 0777 (1935).
4. Mermin, N. D. Hidden variables and the two theorems of John Bell. *Rev. Mod. Phys.* **65**, 803 (1993).

5. Bell, J. S. On the problem of hidden variables in quantum mechanics. *Rev. Mod. Phys.* **38**, 447 (1966).
6. Peres, A. Two simple proofs of the Kochen-Specker theorem. *J. Phys. A* **24**, L175 (1991); *Quantum Theory: Concepts and Methods*, Chapter 7. (Kluwer, 1993).
7. Conway, J. H. & Kochen, S. in *Quantum [Un]speakables: From Bell to Quantum Information*, edited by Bertlmann, R. A. & Zeilinger, A. (Springer-Verlag, Berlin, 2002), P.257.
8. Klyachko, A. A., Can, M. A., Binicioglu, S. & Shumovsky, A. S. Simple test for hidden variables in spin-1 systems. *Phys. Rev. Lett.* **101**, 020403 (2008).
9. Cabello, A. State-independent quantum contextuality and maximum nonlocality. eprint arXiv:1112.5149.
10. Huang, Y. F., Li, C. F., Zhang, Y. S., Pan, J. W. & Guo, G. C. Experimental test of the Kochen-Specker theorem with single photons. *Phys. Rev. Lett.* **90**, 250401 (2003).
11. Hasegawa, Y., Loidl, R., Badurek, G., Baron, M. & Rauch, H. Quantum Contextuality in a Single-Neutron Optical Experiment. *Phys. Rev. Lett.* **97**, 230401 (2009).
12. Bartosik, H., Klepp, J., Schmitzer, C., Sponar, S., Cabello, A., Rauch, H. & Hasegawa, Y. Experimental Test of Quantum Contextuality in Neutron Interferometry. *Phys. Rev. Lett.* **103**, 040403 (2009).

13. Kirchmair, G., Zahringer, F., Gerritsma, R., Kleinmann, M., Guhne, O., Cabello, A., Blatt, R. & Roos, C. F. State-independent experimental test of quantum contextuality. *Nature* **460**, 494 (2009).
14. Moussa, O., Ryan, C. A., Cory, D. G. & Laflamme, R. Testing contextuality on quantum ensembles with one clean qubit. *Phys. Rev. Lett.* **104**, 160501 (2009).
15. Lapkiewicz, R., Li, P., Schaeff, C., Langford, N. K., Ramelow, S., Wieśniak M. & Zeilinger, A. Experimental non-classicality of an indivisible quantum system. *Nature* **474**, 490 (2011).
16. Zu, C., Wang, Y. X., Deng, D. L., Chang, X. Y., Liu, K., Hou, P. Y., Yang H. X. & Duan, L. M. State-independent experimental test of quantum contextuality in an indivisible system. eprint arXiv:1207.0059.
17. Gruber, A. *et al.* Scanning confocal optical microscopy and magnetic resonance on single defect centers. *Science* **276**, 2012 (1997).
18. Jelezko, F., *et al.* Observation of coherent oscillations in a single electron spin. *Phys. Rev. Lett.* **92**, 076401 (2004).
19. Gaebel, T. *et al.* Room-temperature coherent coupling of single spins in diamond. *Nature Physics* **2**, 408 (2006).
20. Childress, L. *et al.* Coherent dynamics of coupled electron and nuclear spin qubits in diamond. *Science* **314**, 281 (2006).

21. Jiang, L. *et al.* Repetitive readout of a single electronic spin via quantum logic with nuclear spin ancillae. *Science* **326**, (2009).
22. Neumann, P. *et al.* Quantum register based on coupled electron spins in a room-temperature solid. *Nature Physics* **6**, 249 (2010).
23. Shi, F. *et al.* Room-temperature implementation of the Deutsch-Jozsa algorithm with a single electronic spin in diamond. *Phys. Rev. Lett.* **105**, 040504 (2010).
24. Maze, J. R. *et al.* Nanoscale magnetic sensing with an individual electronic spin in diamond. *Nature* **455**, 644 (2008).
25. Taylor, J. M. *et al.* High-sensitivity diamond magnetometer with nanoscale resolution. *Nature Physics* **4**, 810 (2008)
26. Liu, G. Q., Pan, X. Y., Jiang, Z. F., Zhao, N & Liu, R. B. Controllable effects of quantum fluctuations on spin free-induction decay at room temperature. *Sci. Rep.* **2**, 432 (2012).
27. Pan, X. Y., Liu, G. Q., Yang, L. L. & Fan, H. Solid-state optimal phase-covariant quantum cloning machine. *Appl. Phys. Lett.* **99**, 051113 (2011).
28. Smeltzer, B., Jean McIntyre, J. and L Childress, L. Robust control of individual nuclear spins in diamond. *Phys. Rev. A.* **80**, 050302 (2009).

Acknowledgement This work was supported by NSFC grants (11175248, 10974251) and “973” programs (2009CB929103, 2010CB922904). We would like to thank S.X.Yu and C.H.Oh for useful discussions about

their paper ², we also would like to thank Zu and Zhang from Tsinghua for letting him know their related paper in photonic system ¹⁶ when this manuscript was in preparation. We thank L.M.Duan for discussions.

Author Contributions X.-Y.P., and H.F. designed the experiment. X.-Y.P. is in charge of experiment, H.F. is in charge of theory. Y.-C.C., G.-Q.L., and X.-Y.P. performed the experiment. H.F. wrote the paper, with assistances from X.-Y. Pan, G.-Q.L. and Y.-C.C. All authors conceived the research, analyzed the data and commented on the manuscript.

Competing Interests The authors declare that they have no competing financial interests.

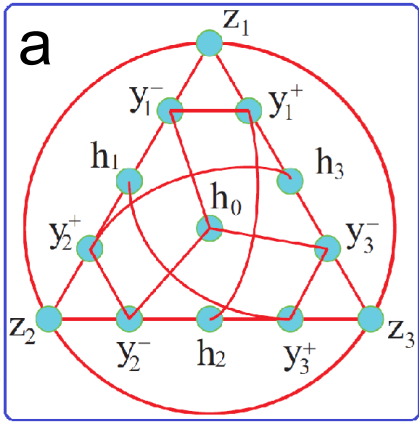
Correspondence Correspondence and requests for materials should be addressed to X.-Y.P or H.F.

Figure 1 The orthogonality relationships among the 13 projection measurement rays. In Yu-Oh version of quantum contextuality proof², the 13 rays, shown in Fig.1(a), are represented by vertices, each connecting bond, curved or straight, between two vertices represents that these two rays are orthogonal and the corresponding observables are compatible (co-measurable) in quantum mechanics. In this scheme, besides that each state should be measured by those 13 observables, there are altogether 24 connecting bonds representing 24 correlations of pairs of compatible observables which should also be measured in our experiment for each input state. To measure the joint probabilities related with correlations, we need additional rays such that we always construct a full basis based on existing 13 projectors. In Fig.1(b), the element in the middle is orthogonal with its row element and column element, so those three states are orthogonal with each other. The forms of those additional vectors are presented in Fig.1(c).

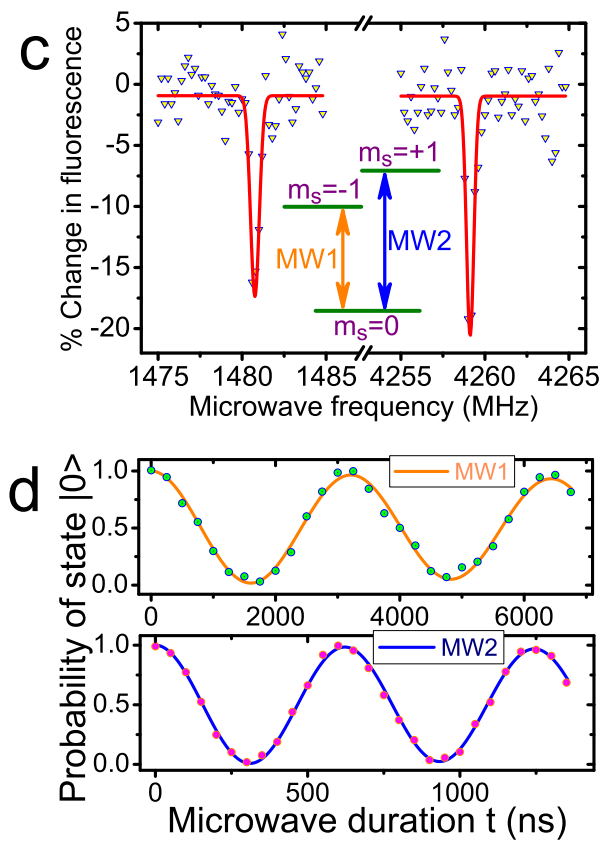
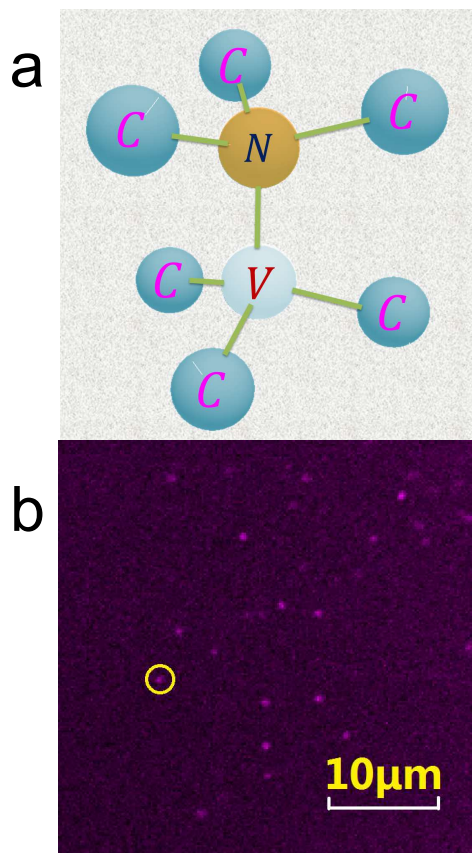
Figure 2 The NV center system in diamond. a. Structure of NV center, a carbon of diamond is replaced by a nitrogen, a vacancy is located in the nearby lattice site. It can offer an electron spin shown quantum phenomena. b. A two-dimensional scan image of NV center, the bright spot (circled) is a NV center which is used in experiment. c. Three energy levels involved in the experiment and their corresponding ODMR spectra, MW1 and MW2 are used to create superposed state between $|0\rangle$ and $|\pm 1\rangle$, respectively. d. Rabi oscillations of MW1 (orange) and MW2 (blue). Those curves are used to find the relative intensity of $|0\rangle$ with $|1\rangle$ and $|-1\rangle$, respectively.

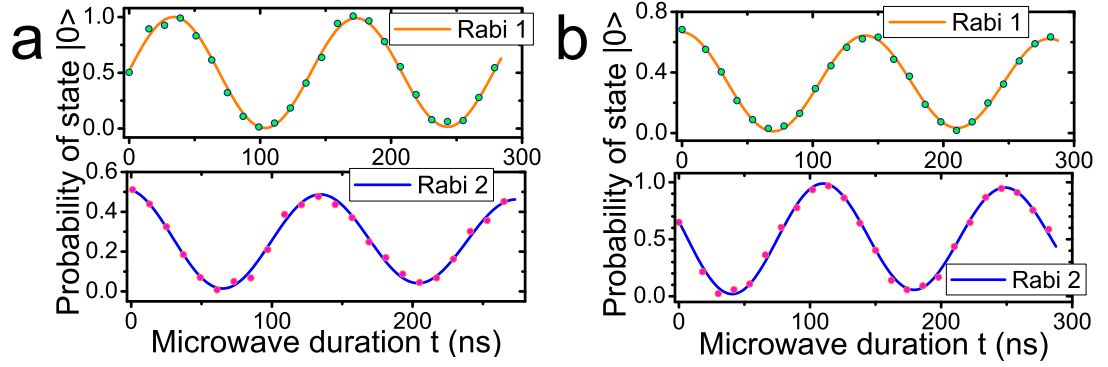
Figure 3 State preparation and projective measurement. Rabi oscillations of MW1 (orange) and MW2 (blue) **a**, on $|y_3^-\rangle$ state and **b**, after projecting $|y_3^-\rangle$ to $|h_0\rangle$ state. **c**, Table: Pulse sequence for state preparation of 13 pure states corresponding to 13 rays and 25 projection readout. Arbitrary qutrits can be prepared, while the measurement scheme is always the same.

Figure 4 Measured results. **a**, we have prepared 13 pure states, each pure state will be measured by 13 observables. Here the theoretical values for those outcomes of observables are presented. In contrast in **b**, the experimental results are presented. Clearly those two figures are almost the same, schematically we show our experimental results agree with theoretical expectations. **c**, as examples, we show the measurement results for three pure states, both theoretical value and experimental values are plotted, they are close to each other. **d**, our summarized results for all prepared 13 pure states, the results range from around 8.1 to around near 8.5, then inequality (1) is always violated without exception. This concludes the experimental test of state-independent quantum contextuality.



C						h_0	$(1,1,1)/\sqrt{3}$	h_1	$(-1,1,1)/\sqrt{3}$	h_2	$(1,-1,1)/\sqrt{3}$	h_3	$(1,1,-1)/\sqrt{3}$
\mathbf{z}_1	$(1,0,0)$	\mathbf{y}_1^+	$(0,1,1)/\sqrt{2}$	\mathbf{y}_1^-	$(0,1,-1)/\sqrt{2}$	\mathbf{x}_1^0	$(-2,1,1)/\sqrt{6}$	\mathbf{x}_1^1	$(2,1,1)/\sqrt{6}$	\mathbf{x}_1^2	$(2,1,-1)/\sqrt{6}$	\mathbf{x}_1^3	$(2,-1,1)/\sqrt{6}$
\mathbf{z}_2	$(0,1,0)$	\mathbf{y}_2^+	$(1,0,1)/\sqrt{2}$	\mathbf{y}_2^-	$(-1,0,1)/\sqrt{2}$	\mathbf{x}_2^0	$(1,-2,1)/\sqrt{6}$	\mathbf{x}_2^1	$(1,2,-1)/\sqrt{6}$	\mathbf{x}_2^2	$(1,2,1)/\sqrt{6}$	\mathbf{x}_2^3	$(-1,2,1)/\sqrt{6}$
\mathbf{z}_3	$(0,0,1)$	\mathbf{y}_3^+	$(1,1,0)/\sqrt{2}$	\mathbf{y}_3^-	$(1,-1,0)/\sqrt{2}$	\mathbf{x}_3^0	$(1,1,-2)/\sqrt{6}$	\mathbf{x}_3^1	$(1,-1,2)/\sqrt{6}$	\mathbf{x}_3^2	$(-1,1,2)/\sqrt{6}$	\mathbf{x}_3^3	$(1,1,2)/\sqrt{6}$





c

State Preparation			Measurement Scheme					
	MW2	MW1		MW1	MW2		MW1	MW2
Z_1	-	-	z_1	-	-	x_1^0	$\cos^{-1}(3/5)$	$\cos^{-1}(2/3)$
Z_2	-	π	z_2	π	-	x_1^1	$2\pi - \cos^{-1}(3/5)$	$\cos^{-1}(2/3)$
Z_3	π	-	z_3	-	π	x_1^2	$2\pi - \cos^{-1}(3/5)$	$2\pi - \cos^{-1}(2/3)$
Y_1^+	$\pi/2$	π	y_1^+	π	$\pi/2$	x_1^3	$\cos^{-1}(3/5)$	$2\pi - \cos^{-1}(2/3)$
Y_2^+	$\pi/2$	-	y_2^+	-	$3\pi/2$	x_2^0	$\pi - \cos^{-1}(3/5)$	$2\pi - \cos^{-1}(2/3)$
Y_3^+	-	$\pi/2$	y_3^+	$3\pi/2$	-	x_2^1	$\pi + \cos^{-1}(3/5)$	$2\pi - \cos^{-1}(2/3)$
Y_1^-	$3\pi/2$	π	y_1^-	π	$3\pi/2$	x_2^2	$\pi + \cos^{-1}(3/5)$	$\cos^{-1}(2/3)$
Y_2^-	$3\pi/2$	-	y_2^-	-	$\pi/2$	x_2^3	$\pi - \cos^{-1}(3/5)$	$\cos^{-1}(2/3)$
Y_3^-	-	$3\pi/2$	y_3^-	$\pi/2$	-	x_3^0	$3\pi/2$	$\pi + \cos^{-1}(1/3)$
H_0	$\cos^{-1}(1/3)$	$\pi/2$	h_0	$3\pi/2$	$\cos^{-1}(1/3)$	x_3^1	$\pi/2$	$\pi + \cos^{-1}(1/3)$
H_1	$2\pi - \cos^{-1}(1/3)$	$3\pi/2$	h_1	$\pi/2$	$\cos^{-1}(1/3)$	x_3^2	$\pi/2$	$\cos^{-1}(1/3)$
H_2	$2\pi - \cos^{-1}(1/3)$	$3\pi/2$	h_2	$\pi/2$	$2\pi - \cos^{-1}(1/3)$	x_3^3	$3\pi/2$	$\cos^{-1}(1/3)$
H_3	$\cos^{-1}(1/3)$	$\pi/2$	h_3	$3\pi/2$	$2\pi - \cos^{-1}(1/3)$			

